FAULT RESISTANCE AND SOIL RESISTIVITY INFLUENCE ON THE IMPEDANCE BASED METHODS FOR LOCATING FAULTS. A COMPARATIVE ANALYSIS

INFLUENCIA DE LA RESISTENCIA DE FALLA Y LA RESISTIVIDAD DEL SUELO EN LOS MÉTODOS DE LOCALIZACIÓN DE FALLAS BASADOS EN LA ESTIMACIÓN DE LA IMPEDANCIA. UN ANÁLISIS COMPARATIVO

JUAN MORA-FLÓREZ
Ingeniero Electricista, Universidad Tecnológica de Pereira, Docente, jjmora@utp.edu.co

GERMÁN GARCÍA-OSORIO
Ingeniero Electricista, Universidad Tecnológica de Pereira, Asistente de Investigación, germangar@utp.edu.co

SANDRA PÉREZ-LONDOÑO
Ingeniero Electricista, Universidad Tecnológica de Pereira, Docente, saperez@utp.edu.co

ABSTRACT: The influence of the soil resistivity and the fault resistance is considered in this paper where a comparison of a well defined impedance based method for locating faults is presented. Tests were performed in a real power distribution system, using soil resistivity measurements and a range of fault resistances commonly found in such systems.

According to the results in a 34kV power distribution system, it is notice that the soil resistivity models which best represents the real systems are those which give better results in the fault location. Additionally, the higher the fault resistance is, the lower the performance index is, showing the influence of this variable. Finally, the influence of the soil resistivity in the distance estimation in such faults where the zero sequence current is different from zero is also analyzed in this paper

KEY WORDS: Fault location, fault resistance, impedance-based methods, soil resistivity.

RESUMEN: En este artículo se analiza de forma comparativa la influencia de la resistividad del suelo y la resistencia de la falla en un método basado en la estimación de la impedancia para localización de fallas. Las pruebas se realizan en un sistema real de distribución, usando medidas de resistividad tomadas directamente en campo, así como valores de las resistencias de falla comúnmente encontradas para estos sistemas de potencia.

Según los resultados en un sistema de distribución de 34,5 kV, los modelos de resistividad que mejor representan a los sistemas reales permiten obtener mejores resultados en la localización de fallas. Adicionalmente, en la medida que el valor de la resistencia aumenta, menor es el desempeño del localizador, lo cual muestra la gran influencia de esta variable. De otra parte, se demuestra la influencia de la resistividad del terreno en la estimación del sitio de falla, en aquellos casos donde existe corriente de secuencia cero.

PALABRAS CLAVE: Localización de fallas, resistencia de fallas, métodos de localización basados en la impedancia, resistividad del suelo.

1. INTRODUCTION

Power systems are commonly exposed to faults caused by a variety of circumstances as lightning, accidental contact with trees or conductive materials, storms, hurricanes, among others. These faults affect the quality of power, reducing the two well known continuity indexes, the System Availability Interruption Frequency Index (SAIFI) and the System Availability Interruption Duration Index (SAIDI) [1, 2]. These indexes are an indirect measure of the maintenance staff response in the case of unpredictable power outages.

Fault location is considered as the first step of a expedite recovery strategy, necessary for maintaining good power service continuity indexes. The fault location task is complex in the case of power distribution systems, mainly due the characteristics of such systems as presence of laterals, tapped loads, multiple conductor gauge, un-transposed lines, single and three phase loads, measurements available only at the power substation, among others [3, 4]. Two additional variables which difficult the accurate estimation of the fault locations are the soil resistivity and the fault resistance [5, 6]. Soil resistivity is commonly ignored or at least assumed as constant along the line route, in most of the real applications which influences the fault location. Fault resistance influences the location due to the difference of the current measured at the power substation and the fault current as it is presented for single phase faults in [7].

Finally, the commonly used methods to determine the fault location are these that use the fundamental of voltage and current measurements at the power substation, to estimate the reactance from the measurement point to the faulted node [6, 8, 9, 10]. However, these methods are influenced by the soil resistivity and the fault resistance, as it is considered and analyzed in this paper. As

contents, this paper presents in section II the fault resistance and the soil resistivity scenarios based in a real power distribution system. Next in section III, the fault location method based on the fault impedance estimation is briefly described. Section IV is devoted to present the test results, while in section V a complete comparison analysis is given. Finally, the main conclusions of the presented research are highlighted.

2. FAULT RESISTANCE AND SOIL RESISTIVITY SCENARIOS

2.1.   Tests system

The system used to analyze the effects of the fault resistance and the soil resistivity, corresponds to a 34,5 kV rated voltage and 157,8 MVA short circuit capability real power system located in Colombia. The circuit is modeled using the alternative transients program (ATP) as it is presented in figure 1 [12].
The aggregated load at the nodes of the main feeder (from Node 1 to node 4), are presented in table 1.

Table 1. Line and load parameters for the test system

Line node	Average load at the main feeder	
	Average apparent power [MVA]	Average power factor
N-1	52,22	0,91
N-2	14,00	0,95
N-3	7,15	0,94
N-4	16,49	0,91

2.2   Line constants estimation

The system impedances corresponding to positive and cero sequences, in per unit length are obtained using equations (1) and (2) [13]. These are derived from the well known Carson theory proposed for considering the effect of the return path [14].
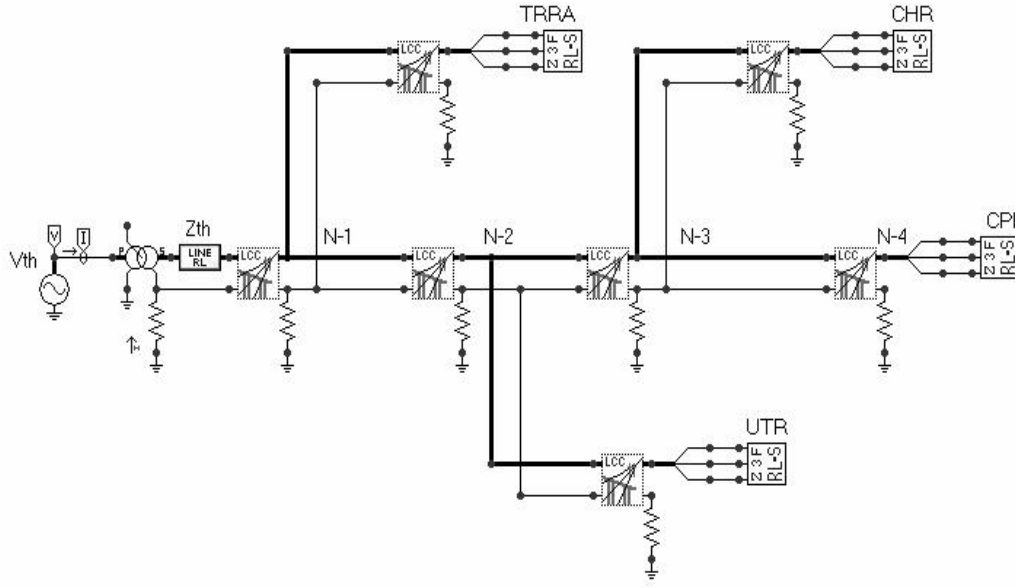
Figure 1. 34kV power distribution system used to test the influence of the soil resistivity and the fault resistance in the fault location

$$R_I = Resistance\ supplied\ by\ the\ manufacturer$$

$$X_L = 2 \times 10^{-4} (2\pi f)\ ln\left|\frac{DME}{RMG}\right|\ \left(\Omega/km\right) \tag{1}$$

$$R_0 = R_{conduc} + 3(0.000988\ f) - \frac{1.015\ f(h_a + h_b + h_c) \times 10^{-6}}{(\rho/f)^{1/2}}\ \left(\Omega/km\right)$$

$$X_0 = 3\left[0.002892\ f\ log\left(\frac{D_e}{r_a}\right)\right] + \frac{1.015\ f(h_a + h_b + h_c) \times 10^{-6}}{(\rho/f)^{1/2}}\ \left(\Omega/km\right) \tag{2}$$

2.2. Soil resistivity scenarios

From the real power distribution system implemented using ATP, it is possible to perform fault simulation of the different fault types considering three different soil resistivity scenarios. The different values are modeled in a low resistivity model (0,01 Ω-m), a zonified resistivity model (Zone 1 of 10,05 Ω-m; Zone 2 of 8,105 Ω-m and Zone 3 of 16.05 Ω-m), and mean resistivity model (11,4 Ω-m). The ground resistivity values for the second model were obtained from field measurements along the line route (44 km length approximately). The impedances estimated using equations (1) and (2) are given in table 2.

Table 2. Resistivity scenarios proposed for the power system in figure 1

Scenario	Section	Length [km]	Series impedance[Ω] Sequence +/-	Sequence 0
Low resistivity	S/E-N1	1,645	0,354+j0,655	0,638+j1,328
	N1-N2	21,26	4,583+j8,475	8,251+j17,164
	N2-N3	13,51	2,913+j5,386	5,244+j10,908
	N3-N4	7,606	1,639+3,032	2.952+j6,141
Mean resistivity	S/E-N1	1,645	0,355+j0,656	0,629+j2,845
	N1-N2	21,26	4,583+j8,477	8,138+j36,77
	N2-N3	13,51	2,913+j5,388	5,173+j23,37
	N3-N4	7,606	1,639+j3,033	2,913+j13,15
Zonified resistivity	S/E-N1	1,645	0,355+j0,656	0,622+j2,702
	N1-N2	21,26	4,583+j8,477	8,039+j34,91
	N2-N3	13,51	2,913+j5,388	5,091+j21,89
	N3-N4	7,606	1,639+j3,033	2,867+j12,32

2.3.   Fault resistance scenarios

To complete the definition of the test scenarios, the four fault types (single phase, phase-to-phase, double phase to ground and three phase) are simulated in all system nodes, considering a variation of the fault resistances from 2Ω to 30Ω [5]. Fault resistances in all affected phases are the same, and the proposed values are 2Ω, 5Ω, 10Ω and 30Ω.

Considering three resistivity scenarios, four fault types and four fault resistances, 48 fault situations are considered at each one of the four nodes of the main feeder. As a result, a database containing 192 fault events is used to perform the proposed comparative study.

3.   PROPOSED IMPEDANCE BASED METHOD FOR LOCATING FAULTS IN POWER DISTRIBUTION SYSTEMS

The impedance based method used to estimate the fault location is presented in this section. This method helps to estimate the fault distance and the fault resistance considering the load flow, the distribution factor and the variation of the source current [8, 9]. The suggested method proposed two different alternatives to determine the fault location: the first one is based on simplified calculations in an iterative nature and the second is based on the solution of a quadratic equation to obtain two unknown variables (the fault distance and resistance). In this research, the second alternative is selected to directly obtain both, the fault distance (m) estimated as a per unit value of the analyzed feeder length and also the fault resistance (R_f).

To estimate m and R_f, a simplification of the power distribution system is proposed. In the simplified circuit, a single load located at the line end as it is presented in figure 2 represents all laterals and tapped loads and the available measurements of voltage and current at the power substation (V_{sf} , I_{sf}). The proposed simplification is then justified considering that the load impedance is bigger than the line impedance, thus the errors caused by load concentration at the main nodes of the main feeder are not significant [8, 15]. However, the

last justification is not always a clear fact, especially in the case of high fault resistances as those here studied [6].
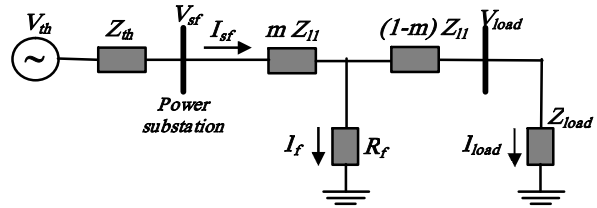
Figure 2 Simplified model of the power distribution system

From the proposed circuit, an equation which considers the voltage and current variations at the steady state of fault and prefault, is derived in terms of m and R_f. The prefault and fault voltage are denoted as V_{ps} and V_{sf}, respectively. Currents are denoted in similar way.

According to the figure 2, the fault distance m is obtained as it is presented in equation (3). I_m indicates the use of only the imaginary parts of the complex variables in brackets.

$$m = \frac{Im\left(\dfrac{V_{sf}}{I_{sf}}\right)}{Im(Z_{l1})} \tag{3}$$

The proposed technique uses pre-fault values of voltage and current to define the superimposed circuit presented in figure 3. This circuit represents the variations caused by the presence of a fault in the circuit shown in figure 2.
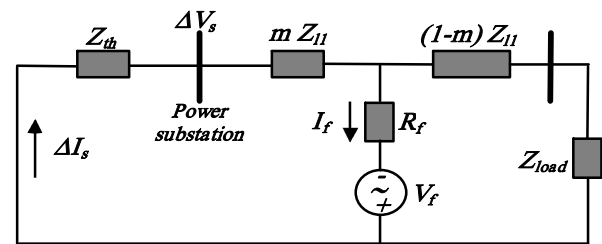
Figure 3 Variations in the voltage and current caused by the fault presence at the power substation of the system depicted in figure 2

From figure 3, the variation in the source current due to the fault is given in equation (4).

$$\Delta I_s = d_s \times I_f \tag{4}$$

Where d_s is the current distribution factor. It describes the variation from the prefault (load current) to the fault current.

The measured apparent impedance, as it is presented in figure 3, is given by equation (5). The factor d_s is obtained from figure 2, as it is presented in (6).

$$Z_{meas} = \frac{V_{sf}}{I_{sf}} = mZ_{l1} + R_f\left(\frac{I_f}{I_{sf}}\right) \qquad (5)$$

$$d_s = \frac{\Delta I_s}{I_f} = \frac{Z_{load} + (1-m)Z_{l1}}{Z_s + Z_{load} + Z_{l1}} \qquad (6)$$

By substituting equation (4) as a function of the fault current in equation (5), the source voltage is given as it is presented in (7).

$$V_{sf} = m\,Z_{l1}\,I_{sf} + R_f\left(\frac{\Delta I_s}{d_s}\right) \qquad (7)$$

Substituting equation (6) in equation (7), equation (8) is then obtained.

$$m^2 - mk_1 + k_2 - k_3 R_f = 0 \qquad (8)$$

Where the constants k_1, k_2 and k_3 are given by (9), (10) and (11), respectively.

$$k_1 = \frac{V_{sf}}{I_{sf} Z_{l1}} + \frac{Z_{load}}{Z_{l1}} + 1 \qquad (9)$$

$$k_2 = \frac{V_{sf}}{I_{sf} Z_{l1}}\left(\frac{Z_{load}}{Z_{l1}} + 1\right) \qquad (10)$$

$$k_3 = \frac{\Delta I_s}{I_{sf} Z_{l1}}\left(\frac{Z_s + Z_{load}}{Z_{l1}} + 1\right) \qquad (11)$$

To estimate the load impedance, equation (12) is then proposed.

$$Z_{load} = \frac{V_{ps}}{I_{ps}} - Z_{l1} \qquad (12)$$

The estimation of the source impedance is performed using equation (13).

$$Z_s = -\frac{V_{sf} - V_{ps}}{I_{sf} - I_{ps}} \qquad (13)$$

Solving the quadratic and complex equation presented in (8), the values of the fault distance m, and the fault resistance R_f are obtained. Finally and having identified the fault type, the values presented in table 3 are then used.

In table 3, k is defined as it is presented in (14), while (15) give ΔIs and finally ΔI_{s1} is obtained as it proposed in (16).

$$k = \frac{Z_{l0} - Z_{l1}}{Z_{l1}} \qquad (14)$$

$$\Delta I_s = I_{sf} - I_{ps} \qquad (15)$$

$$\Delta I_{s1} = I_{sf1} - I_{ps1} \qquad (16)$$

Table 3. Currents and voltages considering the fault type

Fault type	V_{ps}	I_{ps}	V_{sf}	I_{sf}	ΔI_s
a-g	V_{psa}	$kI_0 + I_{psa}$	V_{sfa}	$kI_0 + I_{sfa}$	$3\Delta I_{s1a}$
b-g	V_{psb}	$kI_0 + I_{psa}$	V_{sfb}	$kI_0 + I_{sfa}$	$3\Delta I_{s1b}$
c-g	V_{psc}	$kI_0 + I_{psa}$	V_{sfc}	$kI_0 + I_{sfa}$	$3\Delta I_{s1c}$
b-c	$V_{psb} - V_{psc}$	$I_{psb} - I_{psc}$	$V_{sfb} - V_{sfc}$	$I_{sfb} - I_{sfc}$	$\Delta I_{sb} - \Delta I_{sc}$
a-b	$V_{psa} - V_{psb}$	$I_{psa} - I_{psb}$	$V_{sfa} - V_{sfb}$	$I_{sfa} - I_{sfb}$	$\Delta I_{sa} - \Delta I_{sb}$
c-a	$V_{psc} - V_{psa}$	$I_{psc} - I_{psa}$	$V_{sfc} - V_{sfa}$	$I_{sfc} - I_{sfa}$	$\Delta I_{sc} - \Delta I_{sa}$
b-c-g	$V_{psb} - V_{psc}$	$I_{psb} - I_{psc}$	$V_{sfb} - V_{sfc}$	$I_{sfb} - I_{sfc}$	$\Delta I_{sb} - \Delta I_{sc}$
a-b-g	$V_{psa} - V_{psb}$	$I_{psa} - I_{psb}$	$V_{sfa} - V_{sfb}$	$I_{sfa} - I_{sfb}$	$\Delta I_{sa} - \Delta I_{sb}$
c-a-g	$V_{psc} - V_{psa}$	$I_{psc} - I_{psa}$	$V_{sfc} - V_{sfa}$	$I_{sfc} - I_{sfa}$	$\Delta I_{sc} - \Delta I_{sa}$
a-b-c	$V_{psa} - V_{psb}$	$I_{psa} - I_{psb}$	$V_{sfa} - V_{sfb}$	$I_{sfa} - I_{sfb}$	$\Delta I_{sa} - \Delta I_{sb}$
a-b-c-g	$V_{psa} - V_{psb}$	$I_{psa} - I_{psb}$	$V_{sfa} - V_{sfb}$	$I_{sfa} - I_{sfb}$	$\Delta I_{sa} - \Delta I_{sb}$

4. PROPOSED TEST FOR ESTIMATING THE FAULT DISTANCE

Having defined the soil resistivity and the fault resistance scenarios, the tests of the fault location are performed in all of the defined situations. The results are then presented in this section, considering the proposed soil resistivity scenarios.

4.1. First scenario - Low resistivity model

This scenario is considered due to the common simplification performed in most of the fault location approaches and even in most of the cases of power system fault simulation [3, 10, 15]. According to the tests performed considering a low resistivity model, the results are then presented in table 4.

Table 4. Results of the distance estimation in the case of the low resistivity scenario

Fault type	R_f [Ω]	Real fault distance [km]			
		1,65 (N-1)	22,9 (N-2)	36,4 (N-3)	44,0 (N-4)
Single phase fault (A-g)	2	1,59	22,30	35,60	42,80
	5	1,68	22,50	36,10	44,50
	10	1,70	23,00	36,70	44,70
	30	1,90	24,10	37,90	45,90
Phase to phase fault (A-B)	2	1,65	22,70	36,70	44,70
	5	1,67	23,50	37,40	45,30
	10	1,69	23,50	37,80	46,30
	30	1,72	24,10	38,60	47,00
Double phase to ground (A-B-g)	2	1,68	23,30	37,60	45,30
	5	1,68	23,50	38,00	45,40
	10	1,71	23,10	37,30	45,10
	30	1,72	24,00	38,30	46,50
Three phase fault (A-B-C)	2	1,67	23,10	36,90	44,60
	5	1,67	23,10	37,10	45,00
	10	1,68	23,30	37,30	45,10
	30	1,70	23,80	37,90	46,20

4.2. Second scenario -Mean resistivity model

According to the tests performed in the case of consider a mean resistivity model obtained from the real measurements in field. The results are presented in table 5.

Table 5. Result of the distance estimation in the case of the mean resistivity scenario

Fault type	R_f [Ω]	Real fault distance [km]			
		1,65 (N-1)	22,9 (N-2)	36,4 (N-3)	44,0 (N-4)
Single phase fault (A-g)	2	1,76	23,60	38,60	46,70
	5	1,83	24,10	38,90	46,90
	10	1,89	24,80	39,50	47,70
	30	2,18	25,30	40,20	48,80
Phase to phase fault (A-B)	2	1,65	22,80	36,90	44,70
	5	1,67	23,50	37,40	45,20
	10	1,69	23,60	37,80	46,50
	30	1,72	23,90	38,60	47,30
Double phase to ground (A-B-g)	2	1,66	23,60	37,80	45,60
	5	1,68	23,80	38,10	45,60
	10	1,73	24,10	39,10	47,00
	30	1,76	24,90	39,60	47,87
Three phase fault (A-B-C)	2	1,67	23,20	36,90	44,70
	5	1,68	23,30	37,00	45,20
	10	1,69	23,50	37,50	45,50
	30	1,71	24,20	38,30	46,60

4.3. Third scenario - Zonified resistivity model

According to the tests performed in the case of consider the zonified resistivity model obtained from measurements of the resistivity along the power line route, the results are presented in table 6.

Table 6. Result of the distance estimation in the case of the zonified resistivity scenario

Fault type	R_f [Ω]	Real fault distance [km]			
		1,65 (N-1)	22,9 (N-2)	36,4 (N-3)	44,0 (N-4)
Single phase fault (A-g)	2	1,73	23,1	37,1	44,9
	5	1,78	23,2	37,9	45,8
	10	1,82	23,8	38,3	46,5
	30	2,08	24,9	39,7	48
Phase to phase fault (A-B)	2	1,64	22,8	36,8	44,6
	5	1,66	23,4	37,4	45,2
	10	1,69	23,5	37,9	46
	30	1,72	24	38,5	47,2
Double phase to ground (A-B-g)	2	1,64	23,4	37,2	45,2
	5	1,66	23,6	37,6	45,4
	10	1,69	23,8	38,5	46,8
	30	1,72	24,5	39	47,5
Three phase fault (A-B-C)	2	1,65	23	36,8	44,5
	5	1,66	23,2	37	45
	10	1,68	23,4	37,4	45,3
	30	1,69	24	38,1	46,3

5. COMPARATIVE ANALYSIS OF THE OBTAINED RESULTS

5.1. Estimation of the absolute error

To comparatively evaluate the performance of the fault locator, and then the influence of the soil resistivity and the fault resistance, the absolute error is estimated as it is presented in equation (17) [3].

$$Error = \left| \frac{lenght_{estimated} - lenght_{real}}{lenght_{feeder}} \right| \times 100 \ (\%) \quad (17)$$

Next, errors considering the fault types, all of the three proposed resistivity scenarios and the fault resistance are presented. Figures 4, 5, 6 and 7, present the errors obtained in the case of single phase faults, phase to phase faults, double phase to ground faults and three phase faults, respectively. All of the figures are presented in the same vertical and horizontal scales.
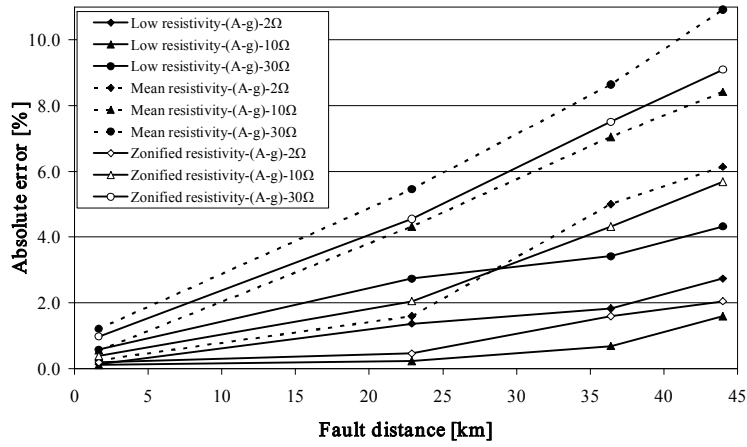
Figure 4 Estimation errors in the case of single phase faults (A-g).
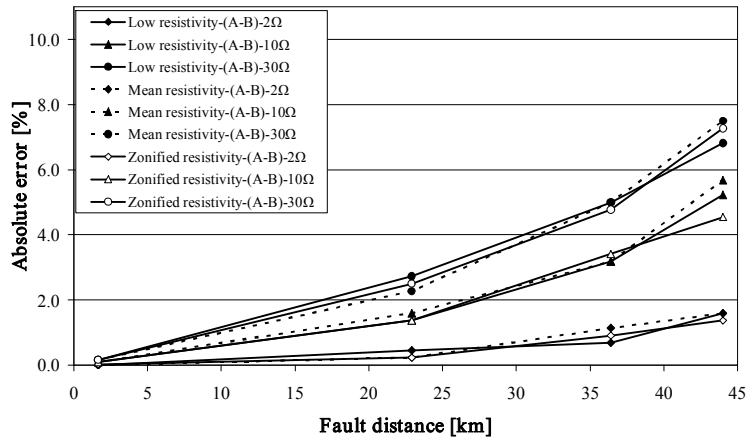
Figure 5 Estimation errors in the case of phase to phase faults (A-B).
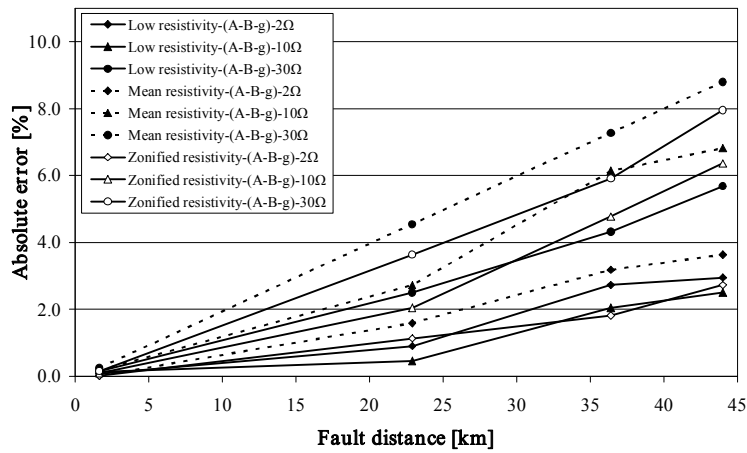
Figure 6 Estimation errors in the case of double phase to ground faults (A-B-g).
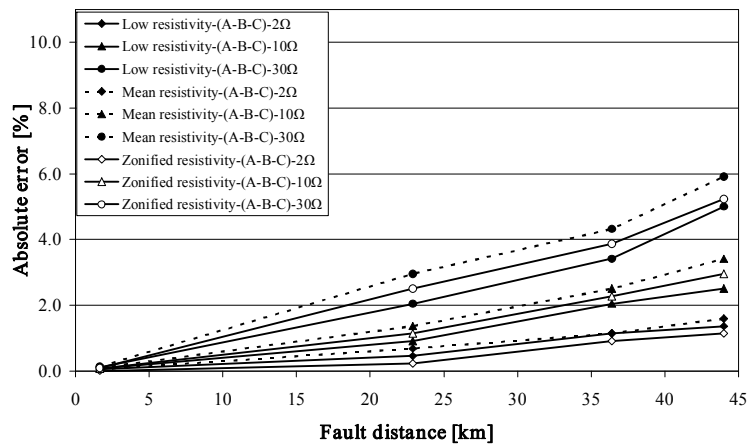
Figure 7 Estimation errors in the case of three phase faults (A-B-C)

5.2.   Analysis of the presented results

Considering the errors obtained as it is presented from figure 4 to figure 7, in the case of the proposed test situations, several considerations are following proposed.

In the case of single phase faults (A-g) as it is presented in figure 4, it is noticed that the mean resistivity model (dotted lines) presents the worst results in all of the error estimations, considering the fault distance and fault resistance. Additionally, it is also noticed how the low resistivity model (neglecting the soil resistivity) presents good results, especially in the case of fault resistance of 10Ω, due to the compensation of the fault resistance and the soil resistivity presented in this particular test case. The fact of not consider the soil resistivity (common assumption), improves the fault location but this result could be particular for the power system used as a test case and is not recommended to generalize it as a common practice. On the other hand, it is notice that the best modeling is the so called zonified resistivity (continuous line and empty geometrical figures) which better represents the real soil resistivity along the power distribution line. Finally, and according to the single phase fault tests, it is noticed the great influence of the fault resistance, which increases the absolute error from approximately 1% to 11%, considering the worst analyzed case (30Ω).

Similar situation to the described for single phase faults is obtained in the case of double phase to ground faults (A-B-g) presented in figure 6, where the most significant errors are obtained in the case of the mean resistivity model. However, lower errors than in the case of single phase faults are obtained in the case of double phase to ground faults, where the worst situation (8.4%) is presented for the mean resistivity model with a fault resistance of 30Ω at the node 4 (44 km).

In the case of phase to phase faults (A-B) and three phase faults (A-B-C) presented in figures 5 and 7, respectively, there is not effect of the soil resistivity as it was expected, due to the non-presence of the zero sequence current in such fault types. According to the obtained errors, it is noticed a similar behavior at the three proposed resistivity models, which only experience changes with the fault distance and the fault resistance. Both of the figures show the influence of the fault resistance and as a consequence the worst situations are obtained in the case of the high consider fault resistance value of 30Ω.

Additionally, considering the error behavior shown in figures 4 and 6 it is noticed how the soil resistivity influences the fault location in such cases where the zero sequence current is involved (ground faults). On the other hand, in the case of phase faults, it is noticed how the error behavior is influenced only by the fault resistance and the fault distance as it is presented in figures 5 and 7. The resistivity model has no influence in the error behavior as it is presented

in the last mentioned figures, confirming in this way the theoretical expected results.

Finally, absolute error is proposed in this paper to adequately compare the deviation from the real fault location in all of the analyzed nodes. Relative error computed using only the real and the estimated distance at the faulted node is adequate to determine the real behavior of the fault locator, but is not useful for comparison.

6. CONCLUSIONS

In this paper, a comparative analysis is presented by considering different soil resistivity scenarios obtained from real measurements, several values of fault resistance and all of the four fault types. According to the obtained results using a well described impedance based fault location method, applied in a real 34,5 kV power distribution system, it is notice the considerable influence of the soil resistivity in the case of ground faults, where the zonified resistivity model is the recommended. Comparing the errors obtained in the case of ground faults (figures 4 and 6) and the errors obtained in the case of phase faults (figures 5 and 7), it is noticed how in the last case there is not any appreciable difference among errors in the three soil resistivity models used in tests. On the other hand, in the case of ground faults it is noticed how the obtained error magnitudes are influenced by the assumed soil resistivity model. These analyses have to be considerer in practical applications, due the demonstrated influence of the soil resistivity model in the performance of fault locators.The fault resistance greatly influences the performance of the fault locator in both of the cases: ground and phase faults, even in the case of methods which consider this variable in the mathematical modeling. On the other hand and according to the obtained results, it is shown how by using a simplified fault location method, a good guest of the fault distance could be obtained.

Finally, the fault location helps to reduce the restoration time by the expedite determination of the faulted node. It helps to reduce the SAIDI and SAIFI continuity indexes for speeding up the restoration task.

REFERENCES

[1] IEEE Std 37.114. "IEEE Guide for Determining Fault Location on AC Transmission and Distribution Lines". Power System Relaying Committee. 2004. pp. 1-36.

[2] SHORT T. "Electric Power Distribution Handbook". CRC press. 2003. pp. 8-16.

[3] MORALES-ESPAÑA G., MORA-FLÓREZ J., PÉREZ-LONDOÑO S. "Classification methodology and feature selection to assist fault location in power distribution systems". Revista Facultad de Ingeniería -Universidad de Antioquia. Vol. 44. 2008. pp. 83–96.

[4] MORA-FLÓREZ J., CARRILLO-CAICEDO G., BARRERA-NUÑEZ V. "Fault Location in Power Distribution Systems Using a Learning Algorithm for Multivariable Data Analysis". IEEE Transaction on Power Delivery. Vol. 22. 2007. pp. 1715-1721.

[5] DAGENHART J. "The 40-Ground-Fault Phenomenon". IEEE Transactions on Industry Applications. Vol. 36. 2000. pp 30-32.

[6] MORA-FLÓREZ J., MELÉNDEZ-FRIGOLA J., CARRILLO-CAICEDO G. "Comparison of impedance based fault location methods for power distribution systems". Electric Power Systems Research. Vol. 28. 2008. pp. 657–666.

[7] GARCIA-OSORIO G., MORA-FLOREZ J., PEREZ-LONDONO S. Analysis of the ground effect in the single phase fault location for power distribution systems. IEEE/PES Transmission and Distribution Conference and Exposition. 2008. pp: 1-6.

[8] NOVOSEL D., HART D., HU Y., MYLLYMAKI J. System for locating faults and estimating fault resistence in distribution networks with tapped loads. 1998. US Patent number 5,839,093.

[9] FENGLING H.; XINGHUO Y., AL-DABBAGH M. Locating Phase-to-Ground Short-Circuit Faults on Radial Distribution Lines. IEEE Transactions on Industrial Electronics. Vol. 54, N.3, 2007, pp:1581 – 1590.

[10] WAN-YING H.; KACZMAREK R. Equivalent Circuits for an SLG Fault Distance Evaluation by Curve Fitting in Compensated Distribution Systems. IEEE Transactions on Power Delivery. Vol 23, Issue 2, 2008. pp:601 - 608 A.

[11] PEREIRA R., DA SILVA L., KEZUNOVIC M. Location of Single Line-to-Ground Faults on Distribution Feeders Using Voltage Measurements. Transmission & Distribution Conference and Exposition: Latin America, 2006. TDC '06. IEEE/PES 2006. pp:1 - 6 .

[12] DOMMEL H. EMTP Theory Book. Second Edition. Vancouver, BC: Microtran Power System Analysis Corporation, 1992. pp. 86-118.

[13] ANDERSON P. Analysis of faulted power systems. The Iowa State University Press. First edition. Fifth printing. 1995. pp. 56-127.

[14] CARSON J.R. Wave propagation in overhead wires with ground return. Bell System Technical Journal, 1926, vol. 5, pp. 539-554.

[15] YANG L. "One terminal fault location system that corrects for fault resistance effects". US Patent number 5,773,980. 1998.